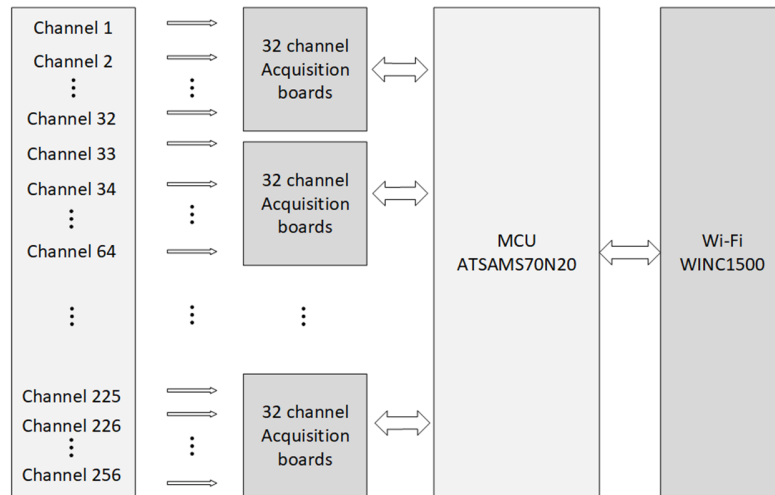


# Supplementary Materials

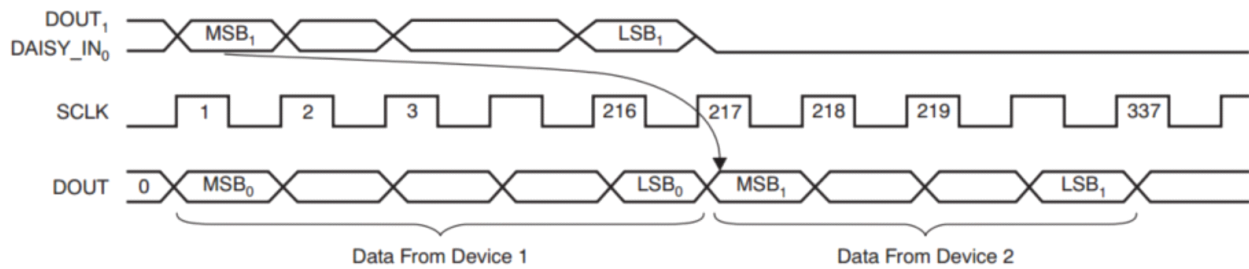
## 1 Supplemental Notes

### 1.1 Supplemental Note 1

In order to achieve high-density acquisition, multiple ADS1299 stacks are required. The third solution is to connect chips in a daisy-chained way, and output data flows among multiple chips and is finally output by the top chip. Therefore, only one SPI interface is required, but the problem is that data output takes a longer time. In this study, the daisy chain method was used to connect multiple ADS1299s together. Considering the problem of increasing data output time caused by daisy chain, a balance was made between the number of SPI ports and the number of daisy chain cascades. In this study, four ADS1299s were connected through daisy chain, and the data collection and transmission period were fixed at 864 SCLK cycles. Using 20 MHz SPI data, the transmission clock can support up to a 23 K sampling rate, which exceeds the maximum data rate of 16 kSPS of ADS1299. Then, the 32-channel acquisition board can be stacked into a higher number of channel acquisition systems, as up to eight can be stacked.



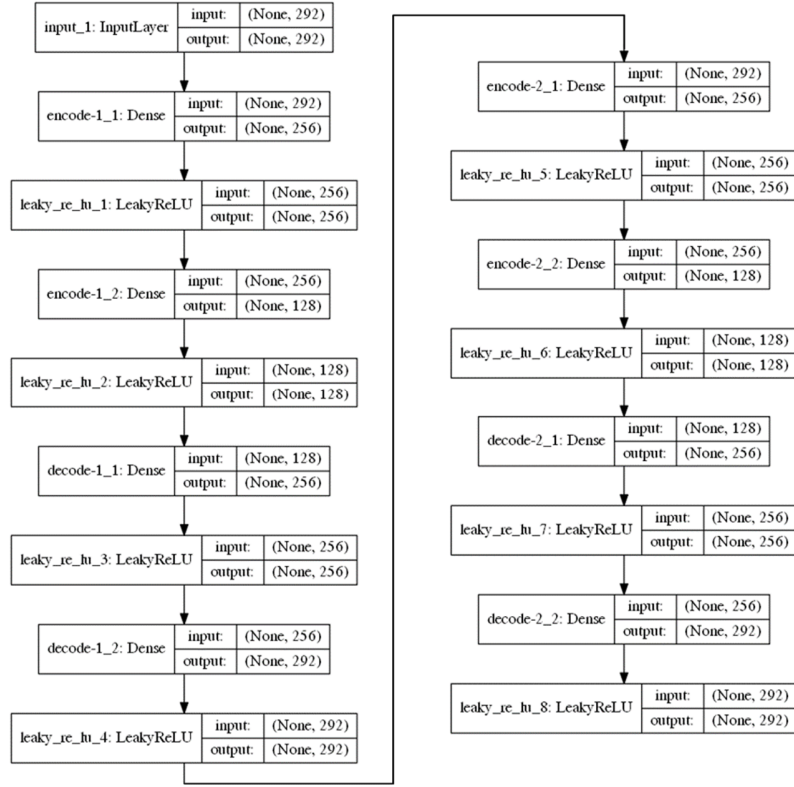
Schematic diagram of the overall acquisition system composition.



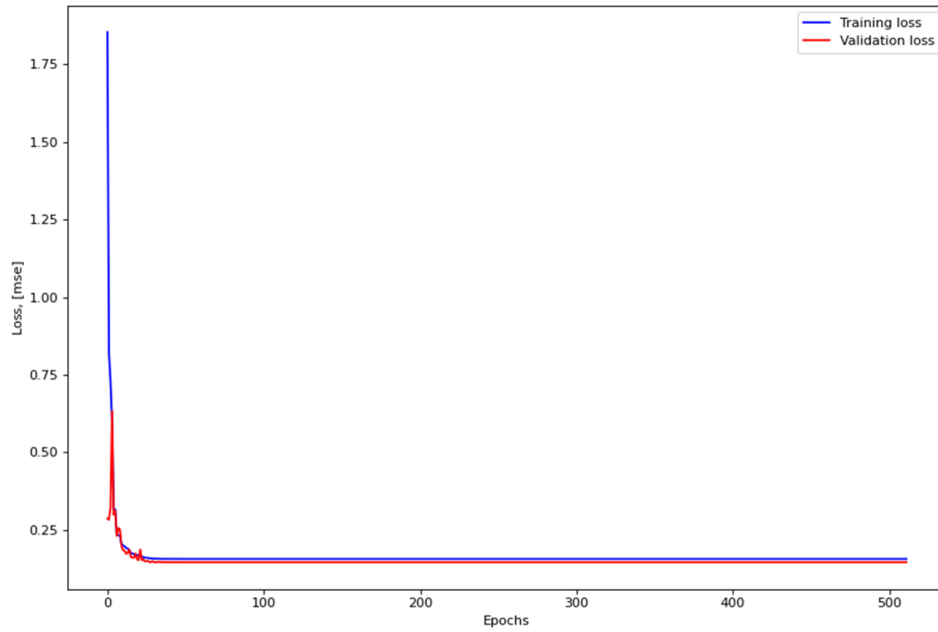
Daisy-chained ADS1299 data sequence diagram.



## 2.2 Supplemental Figure 2



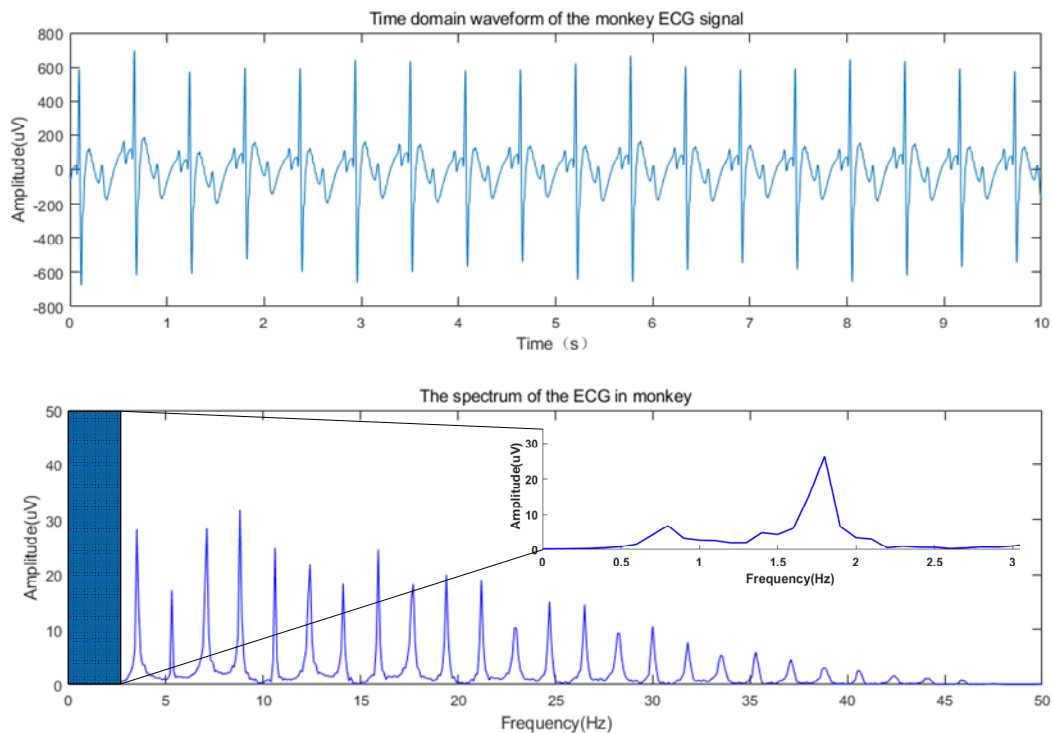
LOGDAE model.



Training and test results of the LOGDAE.

### 2.3 Supplemental Figure 3

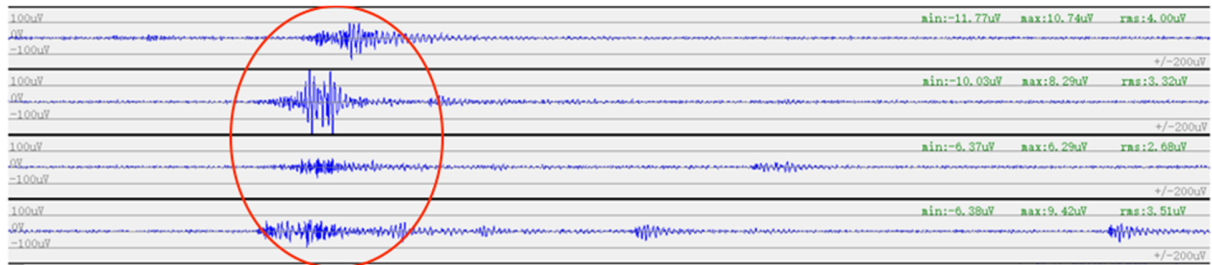
We collected ECG from the monkey outside the MRI room, which was approved by the Animal Ethics Committee. The ECG signals were recorded by differential electrodes with a 1000-Hz sampling rate, and the heart rate was calculated to verify the performance of the ECG recording device. We placed the electrode at the standard ECG position V4, and the signal was collected by the designed system. At the same time, commercially available reflex heart rate monitoring devices monitor heart rates in real time. The signals collected by the system were processed by 50 Hz notch and 0.1 Hz high-pass filtering. The calculated heart rate was 108 per minute, while the commercial reflective heart rate monitoring device showed a heart rate of 110, so the error was within 2%.



ECG recording with a sensor position corresponding to V4.

## 2.4 Supplemental Figure 4

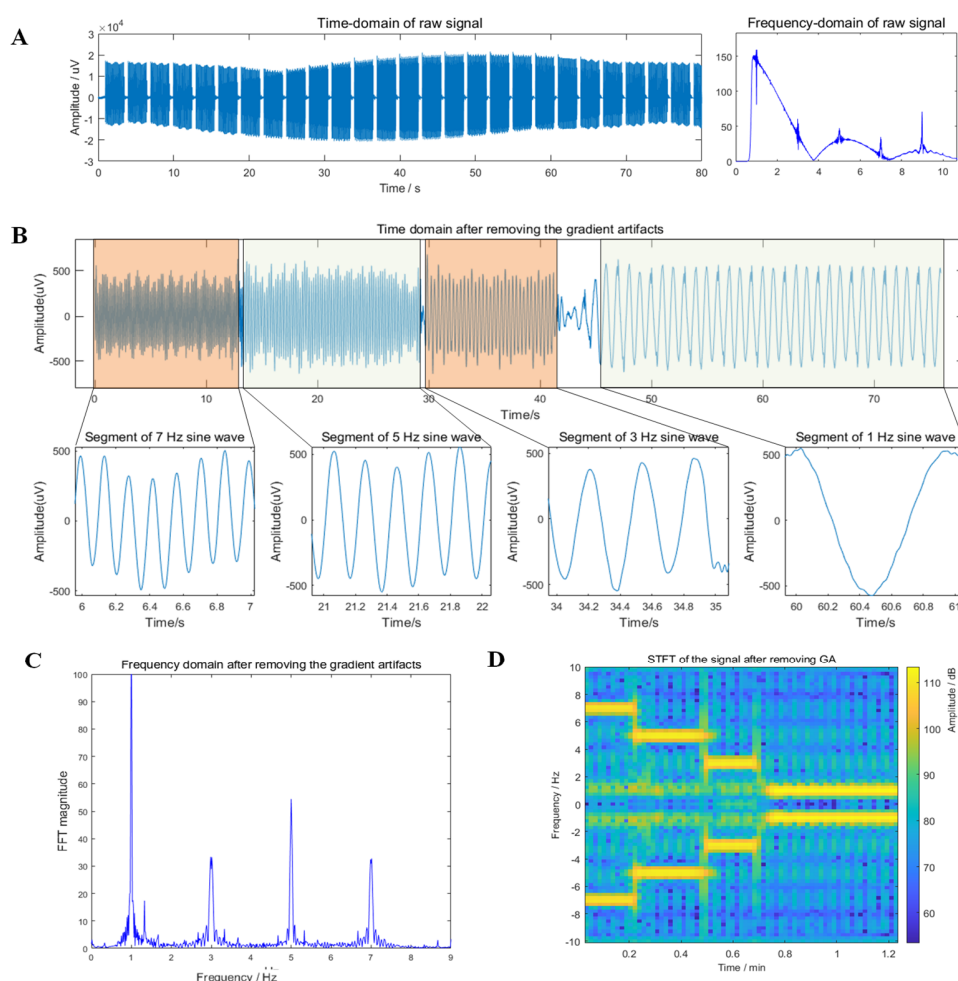
We placed four electrodes on the brachioradialis and brachial flexor of the right arm to record the surface EMG signal when making a fist. The signal was filtered by 20~500Hz bandpass filtering and 50 Hz notch. The results are shown in Figure 7.



Four-channel sEMG recording displayed on the computer user interface for surface EMG recording (The circle represents the moment of force.).

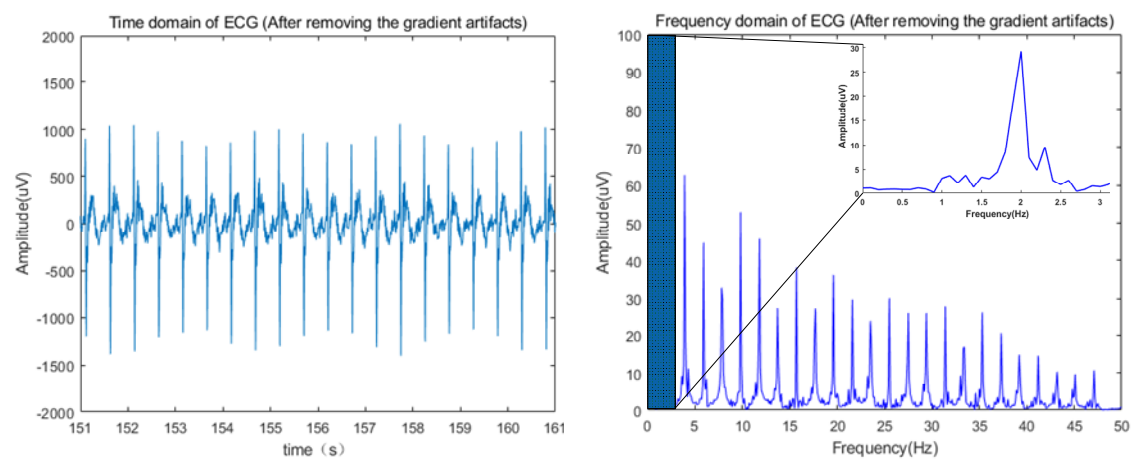
## 2.5 Supplemental Figure 5

We used physiological saline to simulate the brain environment, placed a physiological signal generator outside the MRI room to generate a sine wave signal of a certain frequency and amplitude and introduced the signal into the normal saline within 7T through a carbon fiber wire. One EPI sequence scan was performed for 32 whole brain scans, each with a total brain scan time of 3000 milliseconds and an interval of 500 milliseconds. Each whole brain scan was divided into 25-layer scans with an interval of 100 ms. The PEDOT:PSS electrode collected the sinusoidal signal immersed in the physiological saline, and the MRI scan parameters were set as above. During the MRI scan, we changed the frequency of the physiological signal generator at regular intervals, and the acquisition device collected the sine wave signal in real time.



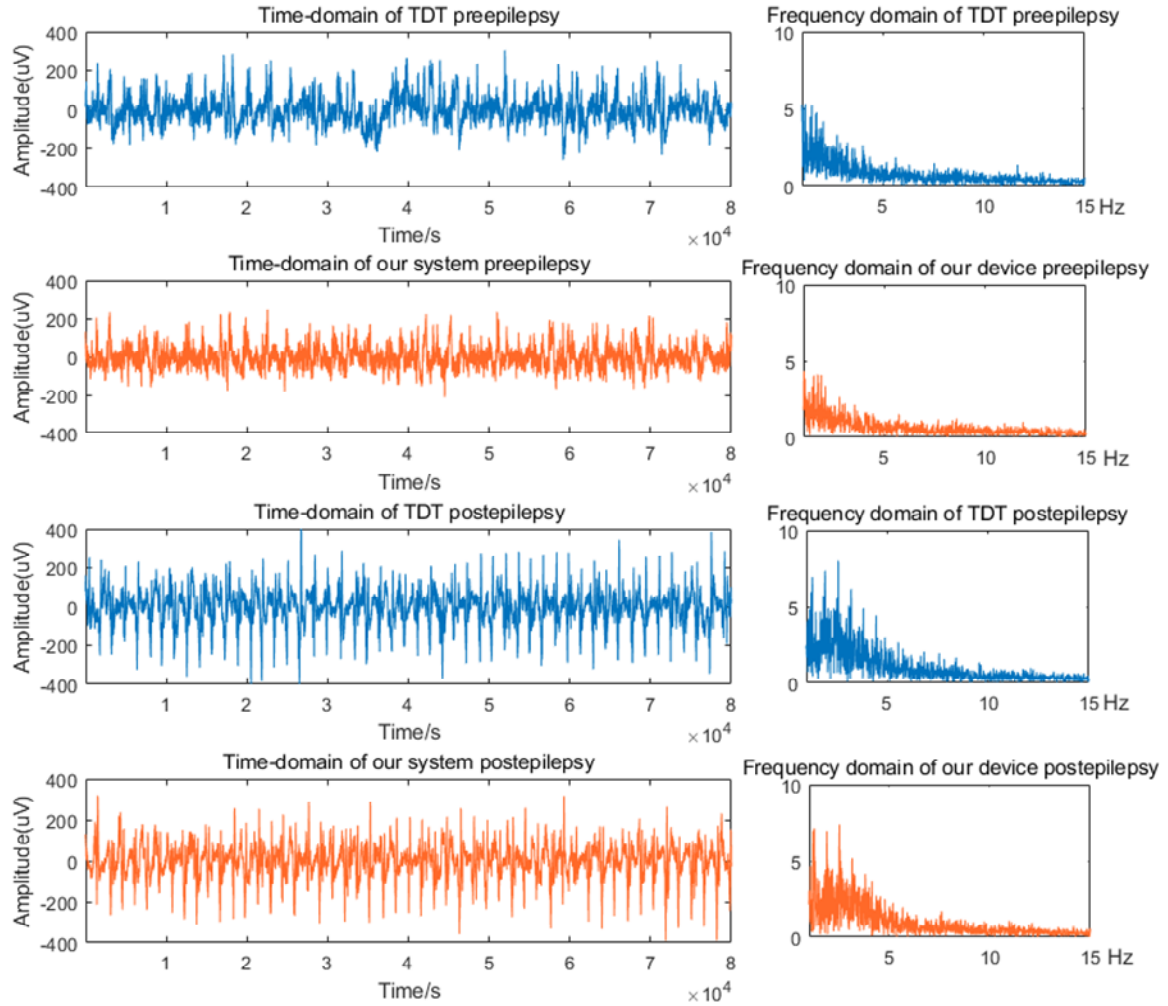
The time domain diagram of the raw signal (The red line indicates the synchronization timing of the MRI scan sequence.). The time domain after removing the gradient artifacts (The figure above represents a time-varying sinusoidal signal with the gradient artifact removed, and below shows the various frequency components of the time-varying signal.) . The time–frequency diagram obtained by short-time Fourier-transform (left is 2D).

2.6 Supplemental Figure 6



Heart rate monitoring by ECG in 7T MRI after removing the gradient artifacts by LOGDAE, the raw data shown in Figure 6.

## 2.7 Supplemental Figure 7



The comparison of normal EEG and epileptic EEG of rats under the non-NMR conditions compared with those signals from the TDT device.



### 3 Supplemental Tables

#### 3.1 Supplemental Table 1

The acquisition device designed in this study achieves 256-channel high-density acquisition and wireless transmission and innovatively integrates EEG and EMG acquisition. Other performance indicators are similar to, or even better than, those of commercial devices. In addition, the system also has magnetic compatibility and a small portable performance.

**Supplemental Table 1.** The performance parameters of our device compared with commercial equipment.

Parameter	Brain Product BrainAmp MR	NeuroScan SynAmps	Delsys Trigno Tiber	NDI-096	Our Device
EP signal compatible	EEG	EEG	EMG	EMG	EEG/sEMG/ECG
Number of channels	32	Up to 256	64-128	4	256
Sample rate	5k SPS	Up to 20k SPS	2k SPS	/	500SPS (256 channel); 16k SPS (8 channel)
ADC bit	16	24	16	24	24
Common-mode rejection rate (CMRR)	-90dB	-110dB	-80dB	-100dB	-110dB
Input noise	<1uVpp	<0.5uVpp	<1.5uVrms	<0.6uVrms	<1uVrms
Bandwidth	0-250Hz	0-3.5kHz	10-450Hz	0.5-10kHz	0-6.8kHz
Input impedance	10M $\Omega$	10G $\Omega$	/	>10M $\Omega$	>500M $\Omega$
Acquisition methods	Single-electrode	Single-electrode/dual-electrode	Single-electrode	Dual-electrode	Single-electrode/dual-electrode

#### 3.2 Supplemental Table 2

**Supplemental Table 2.** Amplitude and frequency ranges of the electrophysiological signal.

Electrophysiological Signal	Amplitude Range (uV)	Frequency Range (Hz)
EEG	1–300	0.1–150
ECG	10–4000	0.1–250
EMG	10–5000	20–1000
ECOG	100–1000	0.1–300
LFP	100–1000	0.1–300